Closed-Loop Actuated Surgical System Utilizing Real-Time *In-Situ* MRI Guidance

Gregory A. Cole, Kevin Harrington, Hao Su, Alex Camilo, Julie G. Pilitsis, and Gregory S. Fischer

Abstract. Direct magnetic resonance imaging (MRI) guidance during surgical intervention would provide many benefits; most significantly, interventional MRI can be used for planning, monitoring of tissue deformation, real-time visualization of manipulation, and confirmation of procedure success. Direct MR guidance has not yet taken hold because it is often confounded by a number of issues including: MRI-compatibility of existing surgery equipment and patient access in the scanner bore. This paper presents a modular surgical system designed to facilitate the development of MRI-compatible intervention devices. Deep brain stimulation and prostate brachytherapy robots are the two examples that successfully deploying this surgical modules. Phantom and human imaging experiments validate the capability of delineating anatomical structures in 3T MRI during robot motion.

1 Introduction

Diagnostic magnetic resonance imaging is one of the most effective imaging modalities available to the medical professional for viewing internal soft tissue structures. The ability to use this modality for live guidance during surgical procedures would prove invaluable for targeting or manipulating internal structures that are difficult to reach for procedures including deep brain stimulation (DBS) and percutaneous prostatic intervention.

Robotic assistance for guiding instrument placement in MRI for neurosurgery began with Masamune, *et al.* [9] and Chinzei, *et al.* [2]. Various methods are utilized to create and control motion within an MRI environment

Gregory A. Cole · Kevin Harrington · Hao Su · Alex Camilo · Julie G. Pilitsis · Gregory S. Fischer
Automation and Interventional Medicine Laboratory,
Worcester Polytechnic Institute, Worcester, MA, USA
e-mail: {gcole,gfischer}@wpi.edu

Julie G. Pilitsis
Albany Medical College, Albany

O. Khatib, V. Kumar, and G. Sukhatme (eds.), *Experimental Robotics*,
Springer Tracts in Advanced Robotics 79,
DOI: 10.1007/978-3-642-28572-1_54,

are utilized, as was outlined by Fischer *et. al.* [5]. The authors have evaluated both pneumatic [4] and piezoelectric approaches [3]. There is additional work being developed in the area of pneumatically actuated robotic devices such as the PneuStep [10]. While this and other pneumatic technology does have a very low level of image interference, the scalability, simplicity, size and inherent robustness of electromechanical systems present a clear advantage over pneumatically actuated systems. A recent piezoelectric approach to prostatic interventions is described by Krieger, *et al.* [8], but as with other published piezoelectric actuation schemes, causes unacceptable image quality loss under motion and must interleave motion with imaging. *While these devices and others in [1, 6] do not depict the entire state of the art, they do highlight the problem being addressed: the current inability to generate and control precision electromechanical motion during live high-field (greater than 1.5T) closed-bore MR imaging without affecting the quality of the image.* The main contributions being discussed in this paper are the system architecture for the rapid development of procedure-specific MRI-guided surgical intervention systems, two example implementations of this system architecture, and experimental validation of their functionality. The two representative procedures targeted are DBS lead placement and prostate brachytherapy.

2 Technical Approach

One of the greatest challenges to creating an MRI-guided robotic system is achieving the required MRI compatibility in terms of safety and image quality [5]. While there are many safety concerns with MRI compatibility in terms of magnetic and conductive materials, employing material restrictions during the design process can easily and effectively minimize these risks. It has been shown that a much more difficult to control compatibility issue is image interference [8, 2]. Most common forms of electronics, especially those containing oscillators, will generate noise in the MR image that will reduce the quality of the images, sometimes to the point that they will not be useful for therapeutic medicine.

Avoiding the high frequency electrical noise problems are very difficult when constructing an MRI compatible system with active motion. A major difficulty in the proposition of constructing an MRI compatible actively driven system is that there are very few "off-the-shelf" products that can be used in the sensitive magnetic environment without destroying the quality of images. The focus of this research is to develop a series of modules that will allow the rapid creation of MR compatible actively driven systems.

2.1 System Architecture

The components of the system presented are specifically constructed for use within an MR scanner and the system is designed to be modular and highly expandable to accommodate a wide variety of needs. As shown in Fig. 1,

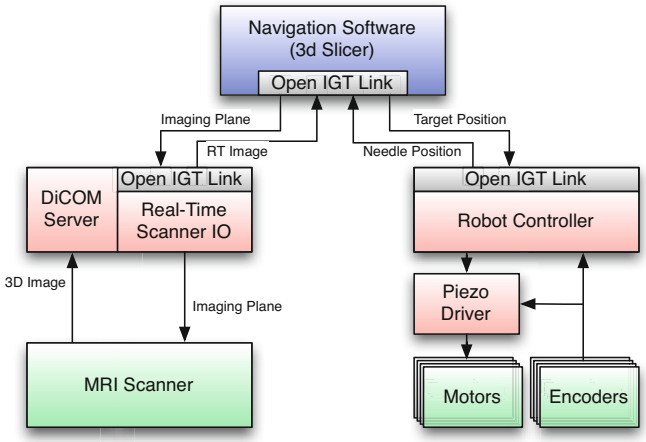

Fig. 1 Architecture of the modular MRI-compatible surgical system.

the architecture is constructed of three primary components that are independent of the hospital equipment: user workstation, controller, and robotic mechanism. The user workstation (typically a laptop computer) resides in the MRI console room, while the robot controller is in the scanner room and the robotic device operates in the MRI scanner bore. The system is completely portable and not coupled to the scanner room – the only external connections are a fiber optic cable that passes through the waveguide and AC power from the wall sockets in the MRI scanner room.

The user workstation resides in the MRI console room and acts as the primary planning and navigation software interface. The system architecture supports a variety of surgical planning platforms by supporting the OpenIGTLink communication protocol between the workstation and the controller [14]. Using the Slicer navigation software platform as described in [13], MR images are compounded into a three dimensional model which is used for procedure planning and interactive guidance tracking. The workstation communicates with the hospital imaging equipment and is responsible for acquiring the MR images and optionally controlling the scanner.

The navigation software sends target and motion commands to the in-room robot controller, which sends back pose and trajectory information about the robotic mechanism. As configured, the navigation software needs not know the robot kinematics – all commands are passed between the planning workstation and robot controller in patient (i.e. RAS) coordinates. The controller itself houses a majority of the original modules: motor drivers, backplane, power supplies, Faraday cage, and control computer. Typically the control computer within the controller contains kinematic information about the mechanism within the scanner bore, and interprets pose commands from the user workstation into joint commands for the mechanism. It then

sends these position or velocity commands to the motor drivers, via the backplane existed. The drivers then produce power signals to operate actuators in the mechanism, and receives and analyzes encoder information for the corresponding degrees of freedom. Through this system architecture, a varying plurality of degrees of freedom can easily and quickly be integrated into a single system. To increase modularity, the backplane has an ethernet interface that can be directly coupled to the fiber optic media converter (as opposed to the internal embedded control computer) to alternatively allow the higher level kinematic control to be performed on a computer outside the scanner room.

2.2 System Modules

All of the presented original system modules were developed because the authors did not feel that any commercial off-the-shelf (COTS) item that would accomplish the desired task without causing signal degradation in the scanner images. One of the more common methods for creating actuated motion in an MRI is the use piezoelectric actuators due to their inherent non-magnetic mode of operation, and the high degree of precision achievable by the actuators. Unfortunately, the available drivers used to operate these motors, while generally not causing interference by their presence in the scanner, do tend to cause a large amount of image degradation while the motors they drive are being driven [7, 5]. The follow describes the specific custom components of the modular MRI-compatible robotic system, with an example system configuration shown in Fig. 2.

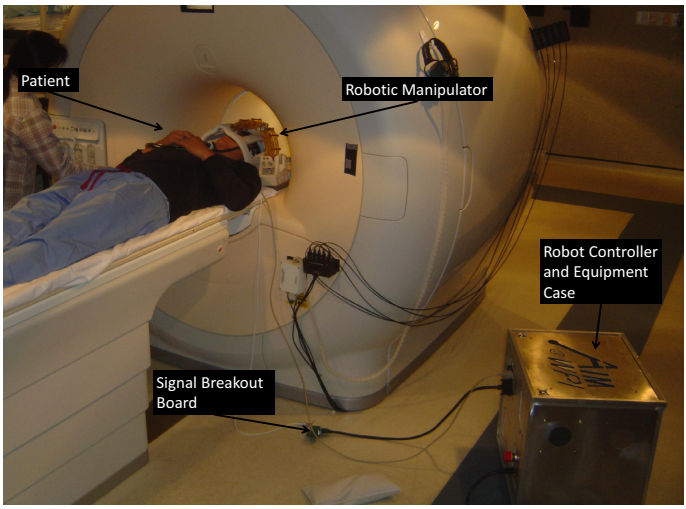

Fig. 2 Example configuration of the robotic system with the controller and other equipment within the scanner room.

Piezoelectric Actuator Driver. The goal was to create a universal platform for driving a wide variety of piezoelectric actuators with a single unit. There are many shapes and forms of piezoelectric actuators, and they generally fall into two major categories: harmonic and non-harmonic. Harmonic motors, also known as ultrasonic motors, generally operate at higher speed and lower torque than non-harmonic motors, and utilize high voltage (200-300 volt) driving waveforms at high frequency (30-50kHz). Some examples of these motors are the Shinsei ultrasonic motor as described in [2], and the Nanomotion HR series of motors described in [8]. While typically the drivers created for these motors output simple sine waves, it was desired to have the ability to finely control the shape of the output waveform to optimize mechanical performance and MR compatibility. In order to accommodate the fine tuning of motor performance, the piezoelectric driver board was constructed with an FPGA-based very high speed (12 mega-samples per second per channel) arbitrary waveform generator, coupled to a high current linear output stage, which is operated with a separate independent power rail. The high degree of precision allows the user to control high frequency signal components being passed through the output stage, which could be expressed as noise or artifacts in scanner images.

While non-harmonic motors, operate at a much lower frequency than harmonic motors (750Hz to 3kHz) they require a high precision non-sinusoidal waveform to operated most effectively. Examples of these waveforms are shown in Fig. 3. Because the shape of the driving waveforms for non-harmonic motors is not a sinusoidal wave, the wave can naturally be broken down into much higher frequency components. Due to the possibility of these components to generate noise in scanner images, precision control of these waveforms is coupled with low-pass filtering on the output. Combining this high speed arbitrary waveform generator and high current output stage with a microprocessor capable of communicating via USB or through the Ethernet backplane allows these driving units to be rapidly integrated into a functional controller. This unit took on the form shown in Fig. 4.

As can be seen from the diagram, the signal processing stage receives an input in the form of a velocity or position setpoint. This signal processing

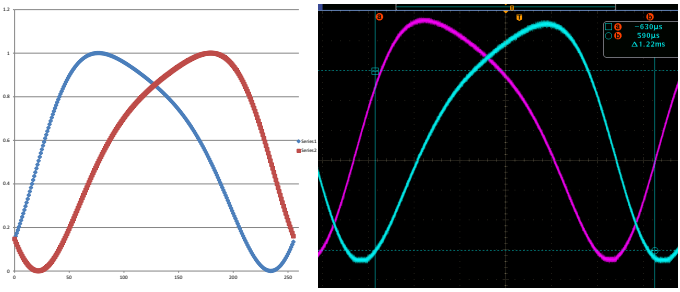

Fig. 3 Example waveforms for non-harmonic motors.

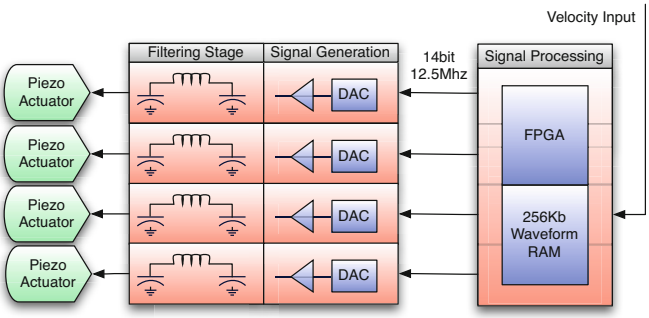

Fig. 4 Configuration of the generalized MR-compatible piezoelectric driver board. The board performs all low-level control and waveform generation and drives up to four piezo elements in a single or multiple motors.

block can then create four independent channels of driving waveforms with a data rate of 12.5 mega samples per second (MSPS) of 14 bit resolution. The signal generators include a high power output amplification stage, which passes its signals out to the actuators through a π filter. The boards also integrate position encoding (from differential encoder receivers) such that closed-loop motion control loops can take place within the FPGA, distributing the real-time processing of the system.

Backplane Signal Aggregator. As has been referenced earlier, a plurality of motor drivers are used for each of the configurations implemented with the system architecture. The software structure of the system uses a single server to interface between the piezoelectric driver boards and the control computer. A PIC microcontroller ethernet device concatenates the lines of communication to and from the controller computer and the driver boards. This functionality is expressed through the backplane connector which contains a series of board edge connecters to plug the drivers into, a socket for the microcontroller ethernet board connector, and output connectors for multiconductor shielded cables. Multiple configurations of the backplane can be customized for the requirements of the particular application. The current system is based on a 10-port backplane with two 68-pin shielded, twisted pair VHDCI cables connecting differential encoder lines and motor power to a distribution block on the robot (5 axes each).

Power Supply. A significant source of noise when attempting to operate electrical equipment within an MR scanner room is switching power converters supplies. One theory is this noise is caused by the high frequency operation, generally on the order of 150kHz to 600kHz) of switching regulators, coupled with their rejection of noise both on the input and the output of the regulators. Because of this, many developers of MR compatible technologies utilize linear regulators (which are highly inefficient), or power supplies external to the scanner room to create DC voltages that are then passed through

the patch panel to supply the in-room equipment (which requires scanner-specific connections and an additional source of noise infiltration). In the proposed architecture, a medical grade linear AC-DC converter generated 48 VDC from the in-room AC supply. To create a power supply that would be capable of operating with a high degree of efficiency (over 85%) while still maintaining MRI compatibility, a switching regulator was designed to operate at a switching frequency of approximately 15kHz, while still maintaining an output ripple voltage under 5 mV. In addition to this, over 15,000 uF of input capacitance was implemented in order to minimize noise that could be rejected on the input to the power supply. The design of this power supply was extensively simulated under varying loading conditions to ensure that it would operate effectively under changing conditions, such as motors switching on and off, or varying computational loads.

Control Computer. The control computer in the in-room controller box in general is expressed as a COTS small form factor computer, that has been modified to be powered off of the supply rails generated by the power supply stages. Previous versions of the controller have used the PC104 form factor, the latest version uses a mini-ITX computer. In general, with a grounded housing and continuous shielded case on a computer such as this, without the original noisy switching power supply, these computers can be operated within the equipment case without much scanner interference [15]. As described earlier, this computer interprets movement and target commands from the user workstation (using the OpenIGTLink) to joint and actuators commands through the use of kinematic information about the mechanism being utilized. In general, this computer communicates to the backplane through an Ethernet socket and to the user workstation through a fiber optic Ethernet connection. To allow a more distributed software architecture, the communication proxy server, trajectory generator, and kinematics engine can be separate applications that communicate over a local network socket. The fiber optic network connection between the control computer and user workstation is utilized to avoid passing any electrical signals through the patch panel which can lead to image interference.

EMI Shielded Enclosure. As discussed before, signal integrity preservation is one of the main difficulties facing the creation of MR compatible robotic systems. A key step in reducing image degradation from electrical noise, is to encase all electronics in a continuous Faraday cage to block as much electromagnetic interference (EMI) being emitted from the equipment as possible. This cage is extended through the shielded cables carrying electrical signals out of the cage. This enclosure is designed to support the modular nature of the system architecture by combining an integrated base of support functionality such as power rail generation and fiber optic communication, with a reconfigurable equipment area as shown in Fig. 5. By making it easy to change out the equipment and system modules within this case, new devices can be integrated and tested streamlining the design process. After the

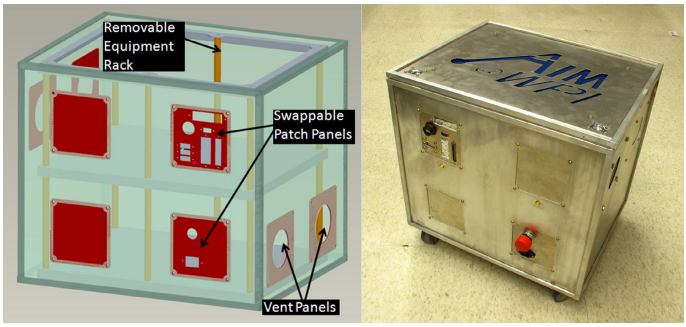

Fig. 5 Solid model of enclosure showing swappable patch panels to allow for different equipment configurations (left) and a photograph of manufactured case (right).

procedure-specific system is tested and verified as functional, a new controller, with dedicated devices can be assembled with a more compact construction.

Tracking Fiducial. One of the challenges implementing image guided surgical procedures, is registering the robotic equipment with the image space. To accomplish dynamic global registration between the robot and the scanner, a passive tracking fiducial frame shown in Fig. 6 is implemented as described in [4]. The construction of this fiducial frame is ABS plastic with seven embedded MR Spot fiducials (Beekley, Bristol, CT). These embedded fiducials form a Z shape in three different planes as shown in 6. By utilizing this arrangement, any arbitrary MR image slicing through all of the rods can provide a full 6-DOF pose of the frame, and thus the robot, with respect to the scanner. By locating the fiducial attached to the robot, the transformation between patient coordinates and the robot's needle driver is known. By transmitting the fiducial's coordinate frame to the robot controller, the end effector location is then calculated from the kinematics based on encoder positions.

Motion Platform. In general, each mechanism is specifically created for a given procedure. Typically a prismatic linear motion is required when placing

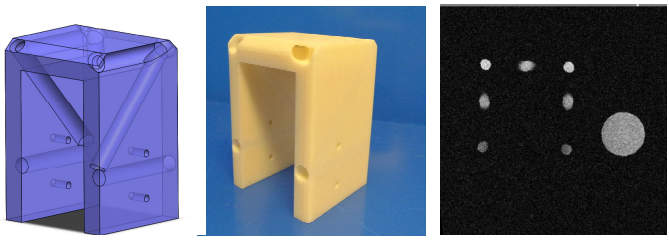

Fig. 6 Left: Solid model of tracking fiducial frame, Middle: tracking fiducial frame used in experiment, Right: Once slice of tracking fiducial frame beside a phantom.

the base point of that mechanism to an appropriate location in image space with reference to the patient. Because of the expected repeated necessity for an X-Y-Z type translation to locate a procedure-specific mechanism to a desired base point with reference to a patient, a 3-axis translational stage was developed as a system module. The X-Y-Z stage is a compact form factor design, with the two perpendicular horizontal degrees of freedom being actuated by linear piezoelectric motors, and the vertical stage, due to the much higher forces expected to be required, being actuated by a scissor-lift connected rotary motor. This is one example of a base for the application-specific manipulator that can be customized for range of motion and spatial constraints as required.

3 Clinical Applications: Two Example Procedures

As a show of the systems modularity, two example interventional systems are being developed in parallel by our research group targeting two different procedures: prostate brachytherapy and DBS electrode placement. While these procedures are very different, because they are both performed on deep, hard to reach soft tissue structures, they could greatly benefit from MR guidance to improve performance and reduce trauma. Each application has a custom end effector mechanism that plugs into a common system architecture.

Fig. 7 Photograph of the remote center of motion (RCM) linkage portion of the DBS insertion mechanism that couple to the above-mentioned translational motion base.

3.1 DBS Electrode Placement System

The most common target for DBS electrodes, the subthalamic nucleus (STN), is deep within the brain and therefore cannot be directly seen during the procedure. In order to accurately target the STN in a traditional procedure, a

lengthy registration procedure is required during which time the patient is under a considerable amount of motion. Coupled with the fact that the MR images utilized to create the surgical plan were taken before the cranium is punctured and some of the cerebrospinal fluid is removed, there is a clearly an opportunity for tissue shift and registration inaccuracy. In order to combat this registrational difficulty, micro electrode recordings are often used to verify correct electrode placement, though these recordings cannot be made with the DBS electrodes themselves. All of these factors can be reduced to the same problem: there is no *live, in-situ confirmation of electrode location while the electrode is being placed.* Inaccurate placement of electrodes has been shown to cause side effects ranging from procedure ineffectiveness to new psychological symptoms and even death [3]. By giving the surgeon access to interactively updated MR imaging during a procedure, there is an opportunity for greater accuracy, in addition to greatly streamlining and shortening the procedure by bypassing complicated, multi modality registration procedures, and allowing the entire procedure to be performed with the patient remaining in one location. This reduces anesthesia usage, trauma and cost of the procedure as well. The equipment setup for this proposed system is shown in Fig. 7.

This system was constructed utilizing all of the standard modules listed above, with eight actuator drivers corresponding to the eight possible degrees of freedom (DOF). In addition to this, the mechanism was designed and constructed to be kinematically identical to the a Leksell frame, the current standard for DBS electrode insertion, as shown in Fig. 7. By making the new mechanism kinematically equivalent to the currently used technology of the Leksell frame (a 5-DOF device), it is the authors hope to streamline the adoption of the new system into use by making the procedural planning very similar for the new and old systems. Initially, a 5-DOF system is targeted (three translational DOF, two rotational DOF), indicating a manual insertion, though eventually an 8-DOF system will be developed to integrate active insertion control, as well as providing an additional two degrees of rotation at the end effector to increase armature dexterity as seen in 7.

3.2 Prostate Needle Placement System

The needle placement mechanism utilizes the same types of actuators and encoders as the DBS system, thus an identical controller configuration is utilized. This needle placement mechanism, constructed primarily of rapid prototyped ABS plastic and laser cut acrylic, is comprised of two main segments, a 3-DOF needle driving module (insertion, cannula retraction, and needle rotation) and the generalized 3-DOF cartesian positioning module as described in [12, 11]. This system was designed to work in a configuration similar to TRUS-guided brachytherapy, and as such the MRI bore's 60 cm diameter constrains the spread of the legs and limited the width of the robot to

7 cm. The lower motion platform layer provides linear motion from embedded piezoelectric actuators, while the upper needle driver module layer provides cannula rotation and stylet prismatic motion. This structure minimizes the "between leg" space while the lower Cartesian stage takes advantage of the available "under leg" space.

4 Experimental Validation

Phantom Test – Quantitative Study. To date there have been a series of experiments with this system, mainly focusing on the ability of the system to generate and control motion while remaining MR compatible. All of the modules presented earlier have been tested individually and as a whole, to ensure that no aspect of the system creates an unacceptable amount of image interference. The specific scan protocols are the same in [15]. The metric of choice to measure signal loss is signal to noise ratio (SNR) which compares an image section that is expected to be 100% signal with an image section expected to be 100% dark, as can be seen in Fig. 8. The results of the total system demonstrate a very low amount of interference as can be seen in 8, with a normalized SNR never exceeding 2.1% as shown in Table 1.

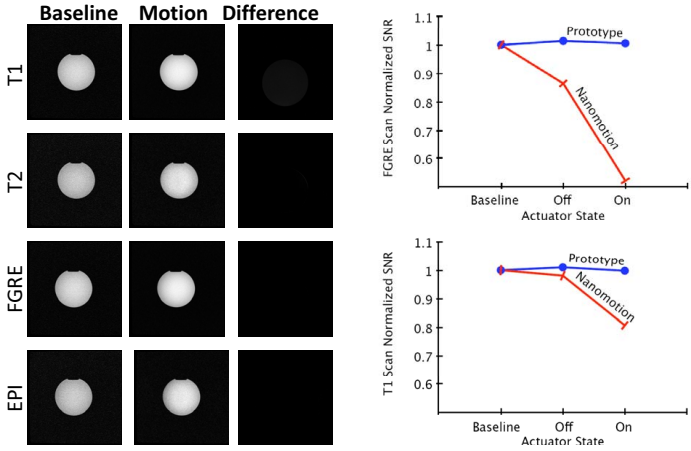

Fig. 8 Left: Image subtraction analysis of interference caused by equipment. Right: Plot of normalized SNR comparing prototype presented in this paper and the one in [8].

Pre-Clinical Evaluation – Qualitative Study. In another series of tests performed, images of a living human subject's brain were acquired during robot motion and shown to several radiologists; the images were determined to be indistinguishable from images taken without any equipment being present in the scanner room. A qualitative demonstration of an operating surgical system on image quality is shown in the anatomy image Fig. 9.

Table 1 Experimental Results of MRI Compatibility Evaluation showing SNR and change percentage

Protocol	**Baseline**	**Motor Off** *(%change)*	**Motor Running** *(%change)*
T1W	148.7	150.5 (1.24%)	149.8 (0.76%)
T2W	620.4	631.8 (1.84%)	629.4 (1.46%)
FGRE	141.2	142.8 (1.19%)	141.6 (0.30%)
EPI	228.4	223.6 (2.09%)	226.3 (0.92%)

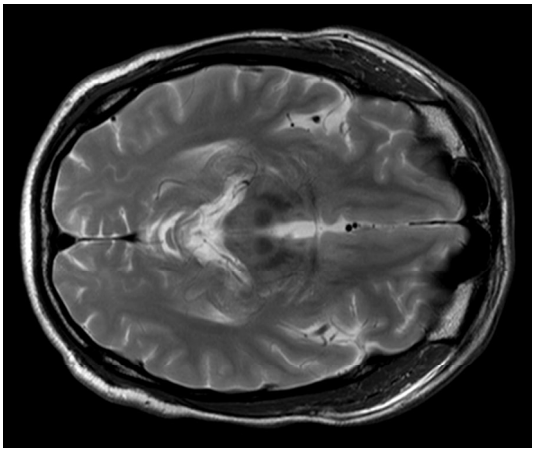

Fig. 9 Clear image of patient anatomy indicating usefulness of images for surgical planning. Note in the image, the lack of background noise.

5 Discussion

It has been shown that the modular surgical system is both capable of creating and controlling motion in an MR scanner without causing image interference, and that the system can be adapted to a multitude of procedure specific mechanisms. Physical performance of the system is to be thoroughly evaluated beginning with robot's precision and clinical ergonomics of the system's configuration. The first phase of this testing will be to determine that accuracy with which the system can move and control its degrees of freedom with reference to itself. The next phase of this testing will be to determine that accuracy with which the system can position itself with respect to image space. Once these performance areas are verified, the system will be tested for ergonomics and usability. After the final rounds of experimental validation discussed in the previous section is completed, these two systems will be moved into cadaver and clinical trials, while new modules and procedures to be incorporated into the modular device set will be pursued. MRI is a highly effective soft tissue imaging system, and the ability to utilize this procedure

in-vivo coupled with precision computer controlled motion will prove to be an invaluable asset in the future development of minimally invasive surgery. The authors hope the presented modular robot controller system will help to expedite the the development of clinically viable MR image-guided robotic surgery systems.

References

1. Carpi, F., Khanicheh, A., Mavroidis, C., De Rossi, D.: MRI compatibility of silicone-made contractile dielectric elastomer actuators. IEEE/ASME Transactions on Mechatronics 13(3), 370–374 (2008)
2. Chinzei, K., Hata, N., Jolesz, F.A., Kikinis, R.: Surgical assist robot for the active navigation in the intraoperative MRI: hardware design issues 1, 727–732 (2000)
3. Cole, G., Pilitsis, J., Fischer, G.S.: Design of a robotic system for MRI-guided deep brain stimulation electrode placement. In: Proc. IEEE Int. Conf. Robotics and Automation, ICRA 2009, pp. 4450–4456 (2009)
4. Fischer, G.S., Iordachita, I., Csoma, C., Tokuda, J., DiMaio, S.P., Tempany, C.M., Hata, N., Fichtinger, G.: MRI-Compatible pneumatic robot for transperineal prostate needle placement. IEEE/ASME Transactions on Mechatronics 13(3), 295–305 (2008)
5. Fischer, G.S., Krieger, A., Iordachita, I., Csoma, C., Whitcomb, L.L., Fichtinger, G.: MRI compatibility of robot actuation techniques–a comparative study. Med. Image Comput. Comput. Assist Interv. 11(pt. 2), 509–517 (2008)
6. Gassert, R., Moser, R., Burdet, E., Bleuler, H.: MRI/fMRI-compatible robotic system with force feedback for interaction with human motion. IEEE/ASME Transactions on Mechatronics 11(2), 216–224 (2006)
7. Kokes, R., Lister, K., Gullapalli, R., Zhang, B., MacMillan, A., Richard, H., Desai, J.: Towards a teleoperated needle driver robot with haptic feedback for RFA of breast tumors under continuous MRI. Medical Image Analysis 13(3), 445–455 (2009)
8. Krieger, A., Iordachita, I., Song, S.E., Cho, N., Guion, P., Fichtinger, G., Whitcomb, L.: Development and preliminary evaluation of an actuated MRI-compatible robotic device for MRI-guided prostate intervention. In: 2010 IEEE International Conference on Robotics and Automation (ICRA), pp. 1066–1073 (2010)
9. Masamune, K., Kobayashi, E., Masutani, Y., Suzuki, M., Dohi, T., Iseki, H., Takakura, K.: Development of an MRI-compatible needle insertion manipulator for stereotactic neurosurgery. J. Image Guid Surg. 1(4), 242–248 (1995)
10. Stoianovici, D., Patriciu, A., Petrisor, D., Mazilu, D., Kavoussi, L.: A new type of motor: pneumatic step motor. IEEE/ASME Transactions on Mechatronics 12(1), 98–106 (2007)
11. Su, H., Camilo, A., Cole, G., Hata, N., Tempany, C., Fischer, G.: High-field MRI compatible needle placement robot for prostate interventions. In: Proceedings of MMVR18 (Medicine Meets Virtual Reality), Newport Beach, California, USA (2011)

12. Su, H., Shang, W., Cole, G., Harrington, K., Fischer, G.S.: Haptic system design for MRI-guided needle based prostate brachytherapy. In: IEEE Haptics Symposium 2010. IEEE, Boston (2010)
13. Tokuda, J., Fischer, G.S., DiMaio, S.P., Gobbi, D.G., Csoma, C., Mewes, P.W., Fichtinger, G., Tempany, C.M., Hata, N.: Integrated navigation and control software system for MRI-guided robotic prostate interventions. Comput. Med. Imaging Graph. 34(1), 3–8 (2010)
14. Tokuda, J., Fischer, G.S., Papademetris, X., Yaniv, Z., Ibanez, L., Cheng, P., Liu, H., Blevins, J., Arata, J., Golby, A.J., Kapur, T., Pieper, S., Burdette, E.C., Fichtinger, G., Tempany, C.M., Hata, N.: Openigtlink: an open network protocol for image-guided therapy environment. Int. J. Med. Robot 5(4), 423–434 (2009)
15. Wang, Y., Cole, G.A., Su, H., Pilitsis, J.G., Fischer, G.S.: MRI compatibility evaluation of a piezoelectric actuator system for a neural interventional robot. In: Proc. Annual Int. Conf. of the IEEE Engineering in Medicine and Biology Society, EMBC 2009, pp. 6072–6075 (2009)